  Bull. Chem. Soc. Jpn., 64, 3229—3244 (1991)

Femtosecond—Picosecond Laser Photolysis Studies on Reduction Process of Excited Benzophenone with Tertiary Aromatic Amines in Acetonitrile Solution

Hiroshi MIYASAKA*, Kazuhiro MORITA, Kenji KAMADA, Toshihisa NAGATA, Manabu KIRI, and Noboru MATAGA*,†
Department of Chemistry, Faculty of Engineering Science, Osaka University, Toyonaka, Osaka 560
(Received April 30, 1991)

Photoreduction processes of benzophenone (BP)-*N*,*N*-diethylaniline (DEA) system in acetonitrile solution were studied by means of femtosecond—pecosecond laser photolysis and time resolved transient absorption spectroscopy. The reaction processes including the formation of geminate ion pairs (IP) by electron transfer (ET) between BP* and DEA at encounter followed by intra-IP proton transfer giving the ketyl radical (BPH·) were clearly observed in both triplet and singlet excited state, while the IP produced by excitation of the CT complex between BP and amine formed easily in more or less concentrated solutions did not give BPH·. In addition to the detailed investigations on the BP-DEA system, we made comparative studies on BP–tertiary aromatic amine systems including *N*,*N*-diethyl-*p*-toluidine, *N*,*N*-dimethylaniline, and *N*-methyldiphenylamine. We observed clearly the characteristic tendency that the proton transfer rate in the ^{3}IP decreased with decrease of the oxidation potential of the amine. This result was interpreted as due to the increase of the inter-ionic distance in the ^{3}IP with increase of the free energy gap for the charge separation at encounter.

Photoinduced electron transfer (ET) and related phenomena play the most fundamental and important roles in many photophysical and photochemical reactions in condensed phase.[1-4] Hydrogen abstraction of excited benzophenone (BP*) from aliphatic as well as aromatic amines in solution is one of the most important photochemical reactions related to this fundamental process and has been extensively studied for a long time.[5-19] Especially, much attention has been paid to the hydrogen abstraction of triplet benzophenone (^{3}BP*), since the rate of the intersystem crossing from the lowest excited singlet state of BP (^{1}BP*) is very large (ca. 10^{11} s^{-1}). On the basis of the experimental results that the yield of the ketyl radical in the reaction of ^{3}BP* with the amine is usually very high and that the reaction rate is rather close to that of the diffusion-controlled reaction, Cohen et al. proposed the following reaction mechanism for the hydrogen abstraction of ^{3}BP* from amines;[7]

$$^3\mathrm{BP}^* + \mathrm{AH} \xrightarrow[\text{transfer}]{\text{Electron}} {}^3(\mathrm{BP}^-\cdots\mathrm{AH}^+) \xrightarrow[\text{transfer}]{\text{Proton}} (\mathrm{BPH}\cdot + \mathrm{A}\cdot)$$

where ^{3}(BP$^-$···AH$^+$) is the CT complex or ion pair, AH is an amine and BPH· is a ketyl radical.

For the more or less direct elucidation of the reaction mechanism, a number of investigations by using laser photolysis methods have been performed on the reduction processes of ^{3}BP*. In an early research by means of a nanosecond laser photolysis,[8,9] it was suggested that the CT or the ion pair (IP) state prior to the solvation was the species undergoing the proton transfer leading to the BPH· formation, i.e., the proton transfer in the IP state competed with the solvation leading to the ionic dissociation.

The direct measurement on the picosecond dynamics of the excited benzophenone and the amine system was reported by Peters and co-workers.[10-13] On the basis of the observed time-dependent spectral shift of the benzophenone anion radical, they concluded that the structural change of the solvent separated IP formed by the ET between ^{3}BP* and the amine to the contact IP was the key process for the proton transfer to take place. Their conclusion, however, rests upon two postulates: (1) The ET reaction proceeds exclusively between ^{3}BP* and amines (AH) even in such concentrated solutions of the amine as 1—5 M, (2) The time dependent spectral shift of the BP anion band is due to the structural change in the IP of BP$^-$ and AH$^+$.

These postulates, however, do not seem valid because of the following facts. First, in addition to formation of the IP by the ET between ^{3}BP* and AH, production of the IP by the ET between ^{1}BP* and AH as well as that from the excited state of the CT complex formed between BP and AH in the ground state are inevitable in such concentrated solutions of the amine. The dynamic behaviors of IP's including their ketyl radical formation, ionic dissociation, etc. the reactivity are strongly dependent on their production pathways even if the donor-acceptor pair and the solvent are the same.[20] The different reactivity of the IP depending on the mode of its production must be taken into considerartion for the elucidation of the reaction mechanism and dynamics of the hydrogen abstraction of excited BP from AH in the concentrated solutions of amines. Second, the dynamic behaviors of these various IP's as well as the dissociated free ions produced in longer time regions (a few hundreds of picoseconds—a few nanoseconds after the excitation) in acetonitrile should be included for the interpretation of

† Dedicated to Professor K. Schaffner on the occasion of his 60th birthday.

the spectral shift, because the spectra of dissociated ions and those of IP's, especially the IP formed by CT complex excitation, are different from each other.

Along this line, we have examined the photoreduction process of excited BP by *N,N*-dimethylaniline (DMA) in acetonitrile solution by means of picosecond and femtosecond laser photolysis.[17,18] From these studies it was revealed that the IP produced by the excitation of the ground state CT complex ($^1IP_{com}$), the IP formed by CS at encounter between $^1BP^*$ and DMA ($^1IP_{enc}$), and that produced by CS at encounter between $^3BP^*$ and DMA ($^3IP_{enc}$) exhibit quite different behaviors including the rate constant of the intra-IP proton transfer (PT) and charge recombination deactivation, etc., dependent on the mode of the production. The PT rate constant of $^3IP_{enc}$ was the largest among those of the three kinds of IP's and the production yield of the ketyl radical of $^1IP_{com}$ was practically zero.

We have reported also the results of the picosecond laser photolysis studies on the reaction of the excited benzophenone with diphenylamine (DPA) in several solvents of different polarity.[16] In this case, it was demonstrated that the hydrogen abstraction and CT or IP state formation by ET reaction were competing at encounter between $^3BP^*$ and DPA both in nonpolar and polar solvent, and the CT or IP state relaxed with respect to the donor acceptor configurations and solvation did not contribute to the ketyl radical formation. Such a direct abstraction mechanism was found to be applicable also in the reaction between $^3BP^*$ and DMA in 2-propanol and in isooctane although the consecutive scheme of the ET followed by intra-IP proton transfer was confirmed for the reaction mechanism in acetonitrile.[18]

In addition, proton abstraction of the dissociated free anion of BP from the neutral amine was responsible for the BPH· formation in the photoreaction of BP–1,4-diazabicyclo[2.2.2]octane (DABCO) in acetonitrile solution,[19] where the PT process within the IP state was not observed.

Various experimental results as described above indicate that the reaction mechanism depends on the structure of the amine and the nature of the solvent. Especially, the experimental findings that the reaction mechanism depends on the solvent even if the same amine is used and that the reactivity of the IP between the same donor and acceptor in the same solvent is different depending on the mode of its production indicate that the mutual distance and orientation, including the surrounding solvents, between BP and AH at encounter are of crucial importance for the subsequent reaction processes.

In the present paper, we report the reduction process of BP* with several tertiary amines, such as *N,N*-diethylaniline (DEA), *N,N*-diethyl-*p*-toluidine (*p*-DET), and *N*-methyldiphenylamine (MDPA), in acetonitrile solution. On the basis of the experimental results obtained by picosecond and femtosecond laser photolysis as well as the previous result with DMA, we discuss the reduction process of the excited BP from the viewpoint of the structure of the transient IP which is determined by the mode of its production and by its energy level.

Experimental

A picosecond laser photolysis system with a repetitive mode-locked Nd^{3+}: YAG laser was used for transient absorption spectral measurements in the 10 ps to a few nanosecond region.[21,22] The third harmonic pulse (355 nm) with 22 ps fwhm or Raman scattering light (397 nm) obtained by focusing the 355 nm pulse into cyclohexane liquid was used for exciting the sample solutions. For the measurement of spectra in shorter time region, a femtosecond laser photolysis system was used.[4,23] In this femtosecond photolysis, second harmonics (355 nm) with 500 fs fwhm of pyridine 1 dye laser (710 nm) was used for the excitation.

Benzophenone (Wako, Special Guarantee) was purified by repeated recrystallization from ethanol and sublimation in a vacuum. *N,N*-diethylaniline (DEA) (Wako, Special Guarantee) was refluxed with acetic anhydride, washed with water, dried over potassium hydroxide, distilled under reduced pressure, and stored under vacuum. *N,N*-diethyl-*p*-toluidine (*p*-DET) (Wako, Practical Grade) was also refluxed with acetic anhydride, washed with water, dried over potassium hydroxide, and distilled under reduced pressure three times. *N*-methyldiphenylamine (MDPA) (Tokyo Kasei, Guaranteed Reagent) was distilled under reduced pressure four times. Acetonitrile (Merck Uvasol) was used without further purification for the time resolved transient absorption spectral measurements. All sample solutions were deaerated by repeated freeze-pump-thaw cycles. The BP solution and DEA were deaerated separately and DEA was added to the BP solution by distillation in a vacuum line. All measurements were performed at 22±2 °C.

The extinction coefficients used for the estimation of the reaction yields are as follows; 6500 M^{-1} cm^{-1} at ca. 525 nm for $^3BP^*$, 4600 M^{-1} cm^{-1} at 545 nm for BPH·, and 10000 M^{-1} cm^{-1} for BP^- around 700 nm. The difference of the extinction coefficient of BP^- ($\leqslant$10%) depending on the solvation and on the state such as ion pair and the dissociated free ion was taken into account in the analysis. Detailed discussion on the determination of the extinction coefficient of each species were presented in the previous paper.[16,18]

Results and Discussion

As mentioned in the introductory section and in the previous papers,[17,18] there exist at least three pathways leading to the IP formation in the photoreduction process of BP by AH:

(1) The excitation of the weak CT complex formed in the ground state, $^1IP_{com}$, (2) The ET reaction between the $^1BP^*$ and the amine, $^1IP_{enc}$, and (3) The ET reaction between $^3BP^*$ and the amine, $^3IP_{enc}$. It is of crucial importance to get precise information on the role played by each IP for the elucidation of the reaction mechanisms of the photoreduction process of BP. From such a viewpoint, we proceed to investigate those problems as

follows.

First, we examine the reaction of ^{3}BP* with DEA leading to the ketyl radical formation and make clear the role of $^3IP_{enc}$ in this reaction. Second, we demonstrate the CT complex formation between BP and DEA in the ground state and the dynamic behaviors of this complex in its excited state. Third, we show results obtained by femtosecond laser photolysis, where the ET reaction of ^{1}BP* and DEA is discussed. By summarizing these results and those obtained for the BP–DMA system,[17,18] we discuss the differences among the reactivities of ^{1}BP*, ^{3}BP*, and three kinds of IP's. Finally, we present the experimental results on the reduction process of ^{3}BP* with *p*-DET and that with MDPA. Based on the results of investigation on the ^{3}BP*–tertiary aromatic amine systems in acetonitrile solutions, we discuss the dependence of the reactivity of the $^3IP_{enc}$ on its structure which seems to be related to the energy gap for the ET reaction producing the IP.

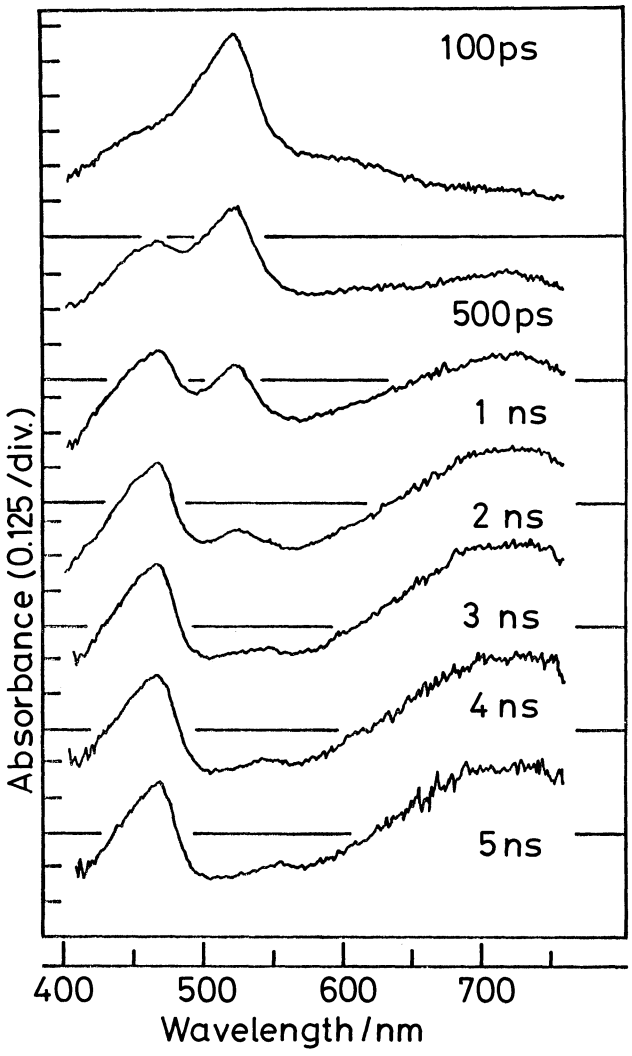

Fig. 1. Time-resolved transient absorption spectra of BP (0.01 M)–DEA (0.05 M) system in acetonitrile solution excited with a picosecond 355 nm laser pulse.

1. Reduction processes of ^{3}BP* by DEA in Acetonitrile Solution. Figure 1 shows the time resolved transient absorption spectra of BP (0.01 M)–DEA (0.05 M) (1 M=1 mol dm^{-3}) system in acetonitrile solution excited with a picosecond 355 nm laser pulse. A transient absorption spectrum with an absorption maximum at 525 nm, which is assigned to ^{3}BP*,[16–19,24,25] decreases with increase of the delay time after the excitation and new bands at 470 nm and ca. 700—720 nm appear. The new absorption band at 470 nm is assigned to DEA$^+$, and that at 700—720 nm to BP$^-$,[26] respectively. Although the absorption signal due to the BPH· radical which has an absorption maximum at 545 nm[27] is observed at longer delay times (3—5 ns) after the excitation, its yield is much smaller than those observed in cases where *N*,*N*-dimethylaniline (DMA) and diphenylamine (DPA) were used as hydrogen donors.[16,17,18] The transient absorption spectra in Fig. 1 indicate that ^{3}BP* gradually evolves with increase of the delay time into BPH· formed by the hydrogen abstraction reaction and $^3IP_{enc}$ produced through the ET reaction. No evolution of the transient absorption spectra was observed at longer delay times than 4 ns after the excitation. Taking into consideration the previous result by nanosecond laser photolysis[9] together with the present one, it may be concluded that the ionic species observed at a few nanosecond after the excitation is due to the dissociated free ions.

In order to clarify time profiles of ^{3}BP*, BPH·, and $^3IP_{enc}$, the observed absorption spectrum at each delay time was analyzed into these three species on the basis of each reference spectrum, the result of which is exhibited in Fig. 2. The ordinate represents the concentration of the individual species calculated by using each extinction coefficient given in the Experimental.

Solid lines in Fig. 2(a) represent the calculated time profiles based on the following scheme, where the BPH· and the $^3IP_{enc}$ which is dissociated into free ions at longer delay times are produced in competition with each other at the encounter of ^{3}BP* with DEA.

$$^3BP^* + DEA \longrightarrow {}^3(BP^-\cdots DEA^+)_{enc} \longrightarrow BP^-_s + DEA^+_s$$
$$\searrow \quad (BPH\cdots DEA\cdot) \longrightarrow BPH\cdot + DEA\cdot$$

Scheme 1.

where DEA· indicates the neutral radical produced after the abstraction of a hydrogen atom from DEA. As is clear from Fig. 2(a), time profile of the BPH· radical and that of $^3IP_{enc}$ could not be well reproduced by Scheme 1. The deviation of the calculated time profile of the $^3IP_{enc}$ from the experimental one in such a way that the experimental result is always larger than the calculated curve in the course of the formation of the IP indicates some rapid deactivation process of the ionic species competing with the ionic dissociation. Moreover, the

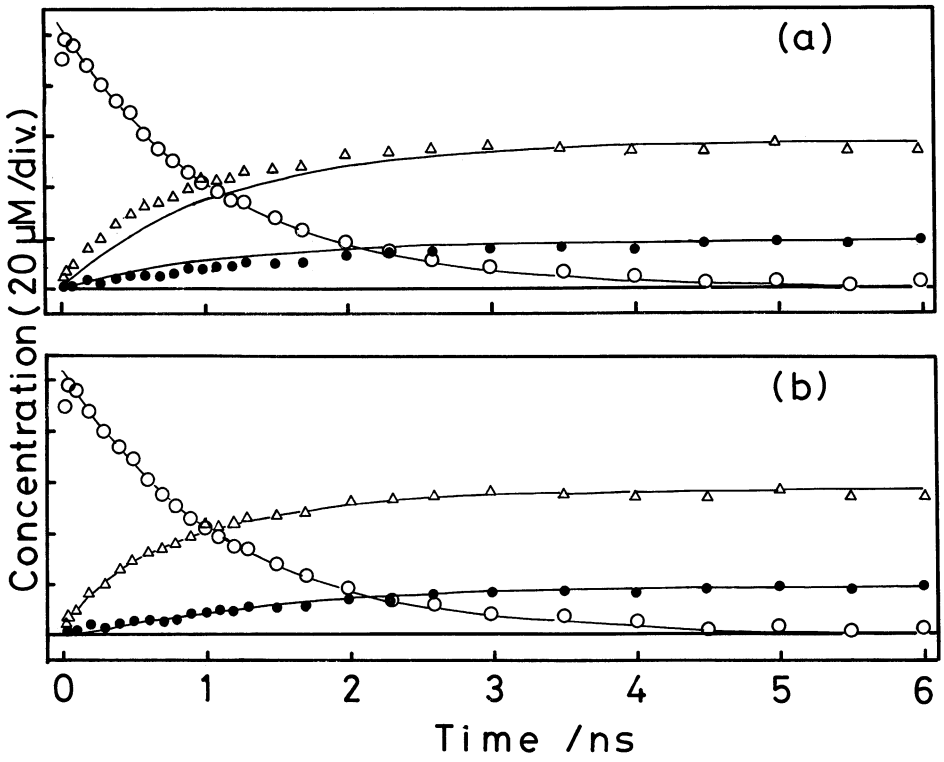

Fig. 2. Time profiles of ^{3}BP* (○), BPH· (●), and BP$^-$ and DEA$^+$ (△) of BP (0.01 M)–DEA (0.05 M) system in acetonitrile solution excited with a picosecond 355 nm laser pulse (see text). Solid lines are calculated curves based on Scheme 1(a), and on Scheme 2(b) (see text).

deviation of the time profile of the BPH· in such a way that the experimental result is always smaller than the calculated curve whose rise time is equal to the decay of ^{3}BP* indicates that the production of BPH· is not directly related to the decrease of ^{3}BP* but some intermediate species exists. Accordingly, the mechanism of Scheme 1 is not adequate for the reaction of ^{3}BP* with DEA in acetonitrile solution, although this direct abstraction mechanism competing with $^3IP_{enc}$ formation was suitable for the hydrogen abstraction process of ^{3}BP* from diphehylamine.[16]

On the other hand, the time profiles calculated on the basis of the Scheme 2 are indicated in Fig. 2(b).

$$^3BP^* + DEA \longrightarrow {}^3(BP^{-}\cdots DEA^{+})_{enc} \longrightarrow BP^-_s + DEA^+_s$$
$$\searrow\ (BPH\cdot\cdots DEA\cdot) \longrightarrow BPH\cdot + DEA\cdot$$

Scheme 2.

Scheme 2 represents the successive mechanism for the hydrogen atom transfer; the IP produced by the ET proceeds to the PT reaction competing with the ionic dissociation process. The parameters for the transient species such as the lifetime of the $^3IP_{enc}$ and reaction yields of the proton transfer and the ionic dissociation were determined respectively in such a manner that the time profiles of ^{3}BP*, BPH·, and $^3IP_{enc}$ were consistent with each other. As shown in Fig. 2(b), the time profile of each species is well reproduced by the calculated curve based on the Scheme 2. The lifetime of $^3IP_{enc}$ was 300 ps and the reaction yield of the proton transfer and that of the ionic dissociation were 0.19, and 0.55, respectively.

In order to confirm the validity of the above parameters obtained by the analysis in Fig. 2(b), we have examined several solutions containing different concentration of DEA. Fig. 3 shows time-resolved transient absorption spectra of BP(0.01 M)–DEA (0.3 M) in acetonitrile solution excited with a picosecond 355 nm laser pulse. ^{3}BP* with its absorption maximum at 525 nm decreases and those of the IP at 470 nm and 700—720 nm, and the BPH· radical at 545 nm increases with increase of the delay time after the excitation. These results are rather similar to those in Fig. 1. However, it should be noted here that the transient absorption spectrum at early stage after the excitation shows a rather large amount of the absorption signal due to IP's compared to that observed in the solution containing 0.05 M DEA. This rapid production of IP's is partly due to the formation of $^1IP_{enc}$, by the ET reaction between ^{1}BP* and DEA, and the formation of $^1IP_{com}$ by the excitation of the CT complex formed in the ground state. More details on these species will be described in the later part of the present paper.

Figure 4 shows the time profiles of three kinds of transient species, ^{3}BP*, BPH·, and IP's, of the BP (0.01 M) –DEA (0.3 M) in acetonitrile solution obtained by the same analysis as in Fig. 2. The initial yield of ^{3}BP* and the sum of yields of IP's which were produced via the excitation of the CT complex and the nonstationary quenching of ^{1}BP* by DEA was in the ratio ca. 3 : 1. In other words, almost 25% of the absorbed photon energy was used for the production of the species other than ^{3}BP*. Solid lines in Fig. 4 are calculated curves based on the consecutive reaction scheme as in Fig. 2(b) and parameters were determined in such a manner that time profiles of these three species were consistent with each other. Contributions from singlet IP's including their lifetimes and reaction yields are included in this calculation, details of which will be discussed later in the present paper.

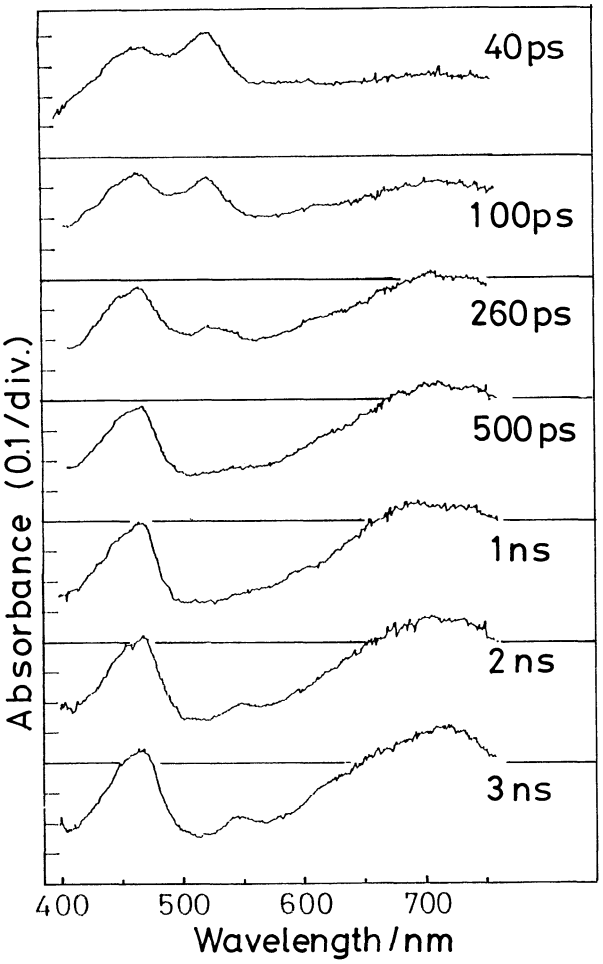

Fig. 3. Time-resolved transient absorption spectra of BP (0.01 M)–DEA (0.3 M) system in acetonitrile solution excited with a picosecond 355 nm laser pulse.

As shown in Fig. 4, experimental results are well reproduced by this calculation with following parameters; the lifetime of $^3IP_{enc}$: 290 ps, the yield of BPH·: 0.23 and that for the ionic dissociation: 0.65. The lifetime and reaction yields of $^3IP_{enc}$ agree with those obtained for the solution containing 0.05 M of DEA (Figs. 1 and 2) within the experimental error.

The consecutive reaction mechanism (Scheme 2) was found to reproduce the experimental time profiles over a wide range of DEA concentration (Table 1). Results in Table 1 clearly show that similar values were obtained for the lifetime and the reaction yields of $^3IP_{enc}$ over a wide range of the concentration of DEA by the curve-fitting procedure, indicating clearly that the reaction mechanism of the hydrogen abstraction of ^{3}BP* from DEA in acetonitrile solution can be described by Scheme 2. Moreover, the rate constant for the ionic dissociation, 2.1×10^9 s^{-1}, was similar to those obtained for a number of organic radical ion pairs produced by the electron transfer at encounter collision in acetonitrile solution at room temperature.[20,28] This result also confirms that the values of the lifetime and reaction yields of the $^3IP_{enc}$ obtained by this analysis and the extinction coefficients used here are appropriate.

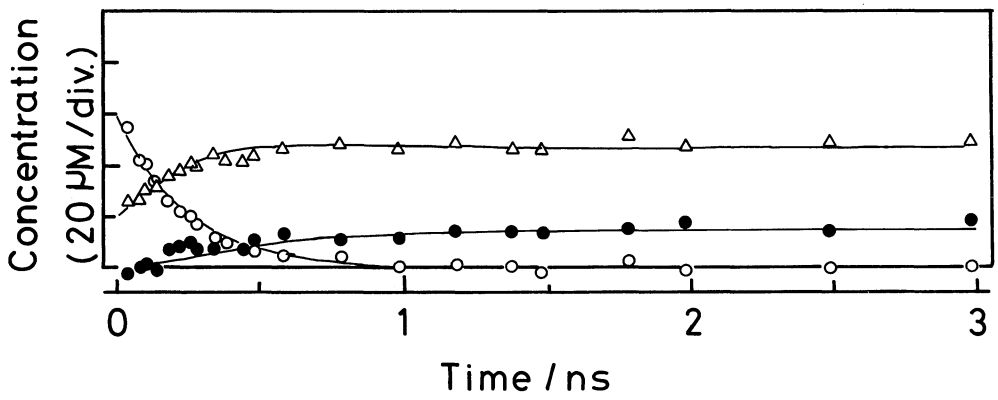

Fig. 4. Time profiles of ^{3}BP* (○), BPH· (●), and BP$^-$ and DEA$^+$ (△) of BP (0.01 M)–DEA (0.3 M) system in acetonitrile solution excited with a picosecond 355 nm laser pulse (see text). Solid lines are calculated curves based on Scheme 2 (see text).

Table 1. Properties of $^3(BP^-\cdots DEA^+)_{enc}$, in Acetonitrile Solutions with Various Concentrations of DEA. τ: Lifetime, ϕ_{PT} and k_{PT}: Reaction Yield and Rate Constant of the Proton Transfer, ϕ_{ID} and k_{ID}: Reaction Yield and Rate Constant for the Ionic Dissociation

[DEA]/M	τ/ps	ϕ_{PT}	ϕ_{ID}	k_{PT}/s^{-1}	k_{ID}/s^{-1}
0.05	300	0.19	0.55	6.0×10^8	1.8×10^9
0.1	280	0.19	0.62	6.8×10^8	2.2×10^9
0.3	290	0.23	0.65	7.9×10^8	2.2×10^9
0.6	290	0.21	0.60	7.2×10^8	2.1×10^9
1.0	270	0.23	0.63	8.5×10^8	2.3×10^9
Average	(286±11)	0.21±0.034	0.61±0.034	$(7.3\pm0.17)\times10^8$	$(2.1\pm0.17)\times10^9$

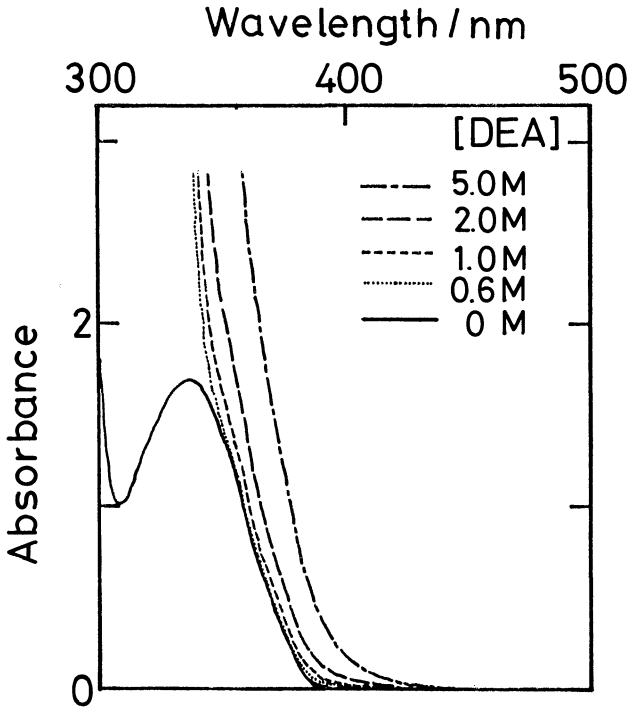

Fig. 5. Effect of DEA concentration on the ground state absorption of benzophenone in acetonitrile.

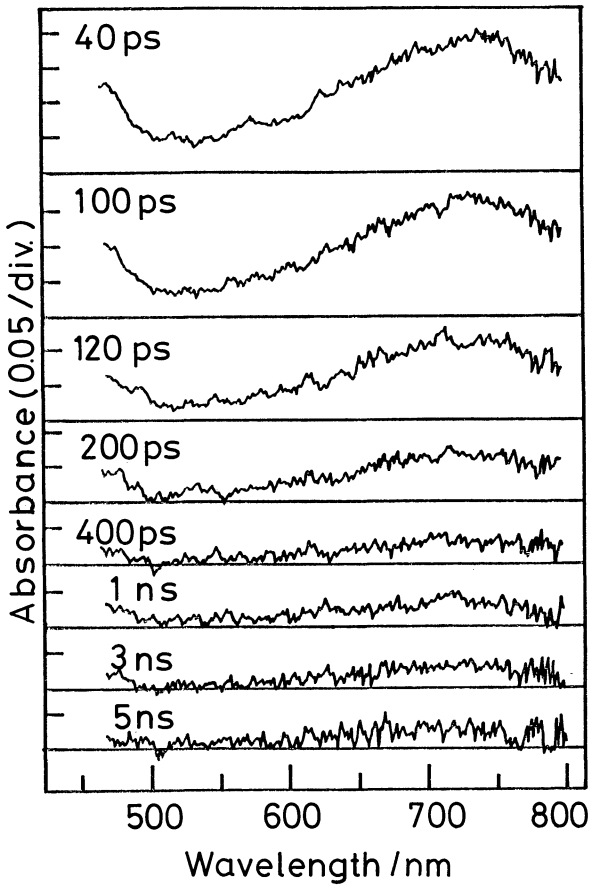

Fig. 6. Time-resolved transient absorption spectra of BP (0.5 M)–DEA (1.0 M) system in acetonitrile excited with a picosecond 397 nm laser pulse.

2. Excited State Dynamics of the Weak CT Complex between BP and DEA Formed in the Ground State in Acetonitrile Solution. In Fig. 5, we show the ground state absorption spectra of BP (0.05 M) with added DEA of various concentrations in acetonitrile solution. The increase of the absorbance in the wavelength region longer than 360 nm was observed with increase of the concentration of DEA. This change of the absorption spectrum can be attributed to the formation of weak CT complex between BP and DEA, since the selective excitation of the absorption tail leads to the immediate formation of $^1IP_{com}$ (see Fig. 6). The equilibrium constant of this complex formation, K_g, was estimated to be 0.1—0.5 by Benesi-Hildebrand plot.

Figure 6 shows transient absorption spectra of BP (0.5 M)–DEA (1.0 M) system in acetonitrile solution excited with a picosecond 397 nm laser pulse, at which wavelength the ground state complex is selectively excited as can be seen from Fig. 5. A broad absorption spectrum with an absorption maximum around 740 nm which appears immediately after the excitation can be safely assigned to BP^- in $^1IP_{com}$ on the basis of the absorption maximum and spectral shape.[18,26] The absorption in the wavelength region shorter than 500 nm, which also appears immediately after the excitation, can be ascribed to DEA^+. With increase of the delay time after the excitation, the absorption due to $^1IP_{com}$ decreases and reaches plateau value attributable to the

dissociated free ions. The decay process of the IP was approximately reproduced by the single exponential function and the time constant was obtained to be (93±5) ps. No absorption due to BPH· was detected after the decay of $^1IP_{com}$. Accordingly, it is concluded that the dominant pathway in the decay of $^1IP_{com}$ is the charge recombination (CR) process and ca. 10% of $^1IP_{com}$ dissociates into free ions.

Similar results to those of the present $^1IP_{com}$ were also observed for the excited state dynamics of the weak CT complex between BP and DMA formed in the ground state in acetonitrile solution.[17,18] Namely, short-lived transient IP state, $^1(BP^-\cdots DMA^+)_{com}$, produced by the excitation at the CT absorption band, was deactivated rapidly via the efficient CR process. The lifetime and the yield of the ionic dissociation of $^1(BP^-\cdots DMA^+)_{com}$ were (85±3) ps and <0.04, respectively. In addition, no BPH· formation was observed also in the course of the decay process of $^1(BP^-\cdots DMA^+)_{com}$. Moreover, the peak position of the absorption band due to BP^- in the IP state, $^1(BP^-\cdots DMA^+)_{com}$, was also at 740 nm, while those of $^3IP_{enc}$ and dissociated free BP^- are around 700—720 nm as shown in Fig. 1. In relation to these results, it should be noted here that the peak position of BP^- absorption changes depending on the structure of the IP and the degree of the solvation according to the previous reports.[29,30] The relation between the peak position of the BP^- absorption and the structure of IP including the surrounding solvents will be discussed in detail in the later part of the present paper.

3. Photoreduction Process of $^1BP^*$ by DEA in Acetonitrile Solution. Figure 7 shows the time resolved absorption spectra of BP (0.05 M)–DEA (0.6 M) system in acetonitrile solution excited with a femtosecond 355 nm laser pulse. The spectrum indicated by the dotted line in the first frame is due to the $S_n \leftarrow S_1$ transition of BP measured in the amine free solution.[17,18] In addition to the $S_n \leftarrow S_1$ absorption spectrum, an absorption maximum at 470 nm and broad absorption whose intensity increases toward longer wavelength region than 600 nm are observed at 1 ps after the excitation of the solution containing 0.6 M of DEA. The absorption band at 470 nm and the broad absorption in the region longer than 600 nm are assigned respectively to DEA^+ and BP^- in the IP. This rapid formation of the IP is due to the excitation at the CT band of the complex overlapping the ground state absorption band of free BP, as stated in the previous section. With increase of the delay time after the excitation, the absorption at 575 nm decreases and the absorption due to the IP gradually increases together with the increase of a new band at 525 nm due to $^3BP^*$.

The time profiles of transient absorbance at 575, 660, and 525 nm are exhibited in Fig. 8. The absorbance at 575 nm due to $^1BP^*$ arises with the time resolution of the apparatus, and shows a rapid decay with the time constant of (5.5±0.5) ps followed by a much slower decay process.

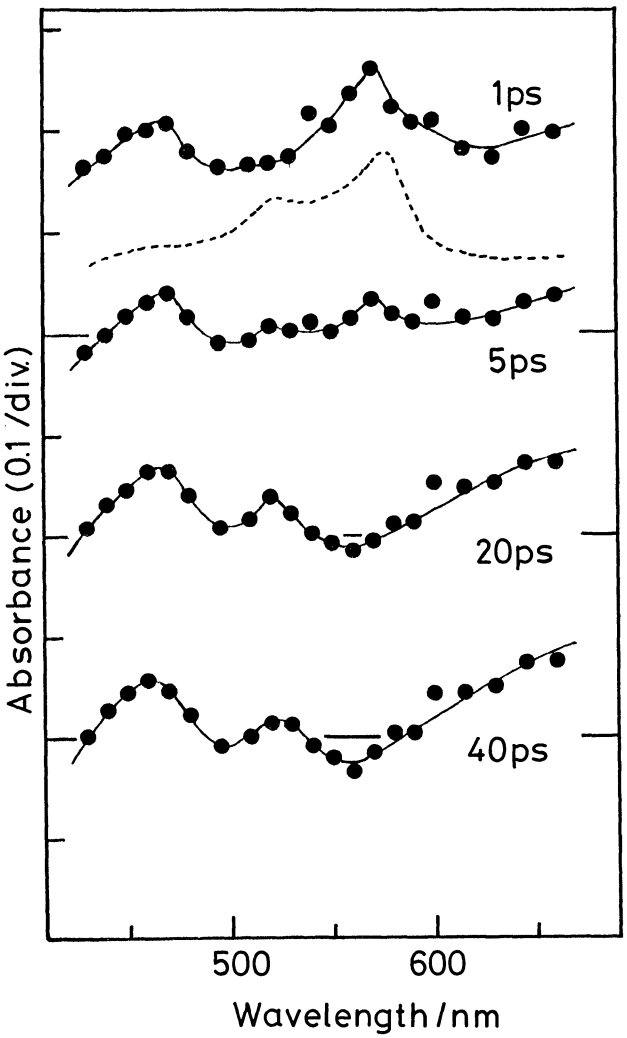

Fig. 7. Time-resolved transient absorption spectra of BP (0.05 M)–DEA (0.6 M) system in acetonitrile, measured by exciting with a 500 fs 355 nm laser pulse.

The rapid decay can be attributed to the quenching process of $^1BP^*$ by DEA on the basis of the time evolution of the spectrum in Figs. 7, 8. Since the lifetime of $^1BP^*$ in amine free solution of acetonitrile was 9.0 ps,[17,18] ca. 30—40% of $^1BP^*$ is quenched by the reaction with the neighboring DEA. On the other hand, the slower decay process with the time constant longer than a few tens of picoseconds may be attributed to the decay of $^3BP^*$ and IP's whose absorptions overlap that of $^1BP^*$ at this wavelength.

The time dependence of the absorbance monitored at 660 nm shows the rapid increase within the response of the apparatus followed by the further increase with the time constant of (5.5±0.3) ps, and then by much slower decay process. The rapid appearance of the IP immediately after the excitation is ascribed to the excitation of the CT complex formed in the ground state. On the other hand, the slower rise with the time constant of (5.5±0.3) ps is due to the IP formation via the ET

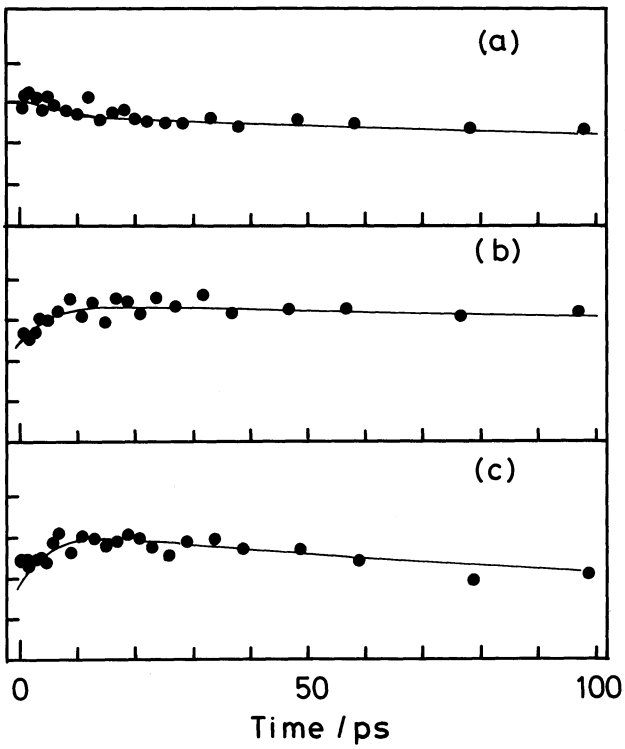

Fig. 8. Time profiles of transient absorbance of BP (0.05 M)–DEA (0.6 M) system in acetonitrile excited with a 500 fs 355 nm laser pulse and observed at 575 nm (a), 670 nm (b), and 525 nm (c).

reaction between ^{1}BP* and DEA, since the time constant of the decrease of ^{1}BP* is identical with the rise time of the IP. The quenching rate constant of ^{1}BP* by DEA, 1.6×10^{11} M^{-1} s^{-1}, is about 8—10 times as large as the diffusion controlled rate constant in acetonitrile. This rapid quenching process is probably due to the rapid reaction of ^{1}BP* with the neighboring DEA, the so-called transient effect or non-stationary quenching. Such a large reaction rate constant for the ET process between ^{1}BP* and the amine was also observed in the case of BP–DMA system.[17,18]

Time profile of the absorbance at 525 nm which is an absorption maximum of ^{3}BP* is shown in Fig. 8(c), indicating that the rapid increase of the absorbance immediately after the excitation is followed by the slower rise and much slower decay process. The rapid rise of the absorbance is ascribed to the contribution of ^{1}BP* as can be seen from Fig. 8(a). The slower increase of the absorbance is ascribed to the formation of ^{3}BP* by the intersystem crossing of ^{1}BP* on the basis of the coincidence of the time constant of the rise of ^{3}BP*, (5.4±0.5) ps, with the decay of ^{1}BP* in Fig. 8(a). Much slower decay of the absorbance may be due to the quenching of ^{3}BP* by DEA and the recombination process of IP's. The rapid quenching process of ^{1}BP* by DEA was also observed in acetonitrile solutions containing 1.0 M of DEA and that with 2.0 M of DEA. The lifetime of ^{1}BP* in the solution of [DEA]=1.0 M was 3.7 ps and that for 2.0 M DEA was 2.5 ps, respectively. With increase of [DEA], the increase of the yield of $^1IP_{enc}$ and the decrease of that of ^{3}BP* were observed.

By the analysis of the transient absorption spectrum immediately after the excitation with the femtosecond 355 nm laser pulse into two components, ^{1}BP* and $^1IP_{com}$, and by dividing each spectrum by the extinction coefficient, the fraction of $^1IP_{com}$ and that of ^{1}BP* were obtained to be 0.33 and 0.67, respectively. The fraction of $^1IP_{com}$ increases with increase of [DEA]. The fraction of $^1IP_{com}$ for 1.0 M solution of DEA and that for 2.0 M solution were 0.38 and 0.67, respectively. In addition, the contribution of the rapid quenching process of ^{1}BP* by DEA also increases with increase of [DEA] and, as a consequence, the yield of ^{3}BP* decreases. From the lifetime of ^{1}BP* and spectral evolution, we can evaluate the initial yields of $^1IP_{com}$, $^1IP_{enc}$, and ^{3}BP*, respectively. For example, only 33% of the light energy absorbed in the acetonitrile solution of BP containing 0.6 M of DEA terminated in the production of ^{3}BP*. This value decreases with increase of [DEA]; that for 1.0 M solution was 25% and that for 2.0 M solution was 10%.

From the above results and discussion, we can summarize the ET and related processes in short time regions of the excited benzophenone in the presence of DEA in acetonitrile solution as follows.

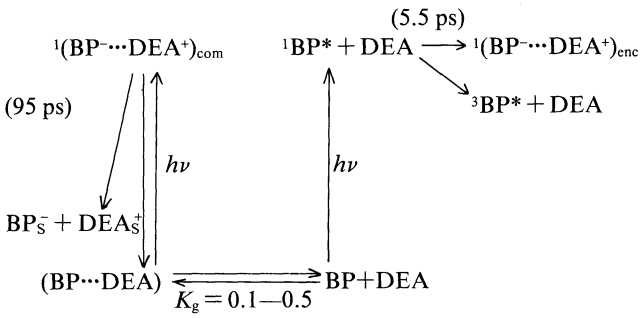

Scheme 3.

In this scheme, the $^1IP_{com}$ produced by the excitation of the CT complex formed in the ground state, is discriminated from the $^1IP_{enc}$ produced via the ET reaction between ^{1}BP* and DEA. In the case of the ET reaction in the system of BP and DMA, clear difference in the reaction processes depending on the mode of the production of IP's was observed between these two kinds of IP's.[17,18] The circumstance was similar also in the present case. The detailed discussion on this difference between two kinds of ^{1}IP's will be given in the later part of the present paper.

In order to elucidate dynamic behaviors and reaction pathways of $^1IP_{enc}$ quantitatively, transient absorption spectra of acetonitrile solutions of BP (0.01 M)–DEA (0.6 M) system in picosecond - a few nanosecond region were measured by means of the picosecond 355 nm laser pulse excitation (Fig. 9). A large amount of transient

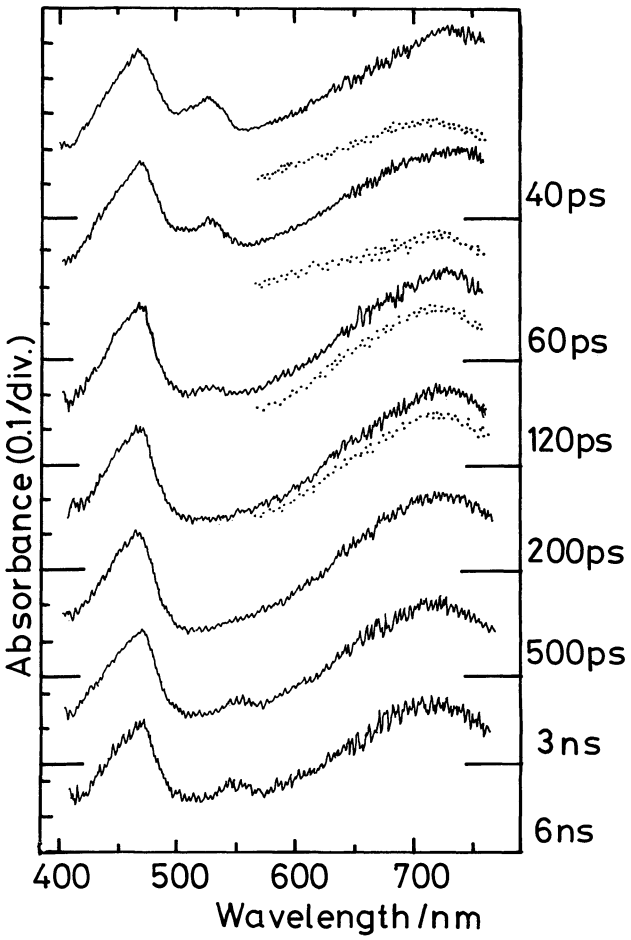

Fig. 9. Time-resolved transient absorption spectra of BP (0.01 M)–DEA (0.6 M) system in acetonitrile solution, excited with a picosecond 355 nm laser pulse. Dotted lines are the absorption spectra obtained by subtracting the contribution of the absorption bands due to $^1(BP^- \cdots DEA^+)_{com}$ from the observed spectra (see text).

absorption due to IP's which involves both $^1IP_{com}$ and $^1IP_{enc}$ was observed immediately after the excitation. In addition to the absorption bands of IP's, clear signal due to the absorption $^3BP^*$ is observed at 525 nm. The initial yield of $^3BP^*$ was 0.33 in this solution containing 0.6 M of DEA as described already in the interpretation of Figs. 7 and 8. With increase of the delay time after the excitation, the absorption of IP's also decreases and reaches a plateau value which is ascribed to the dissociated free ions. Very small absorption signal due to BPH· was observed around 550 nm at longer delay times (3—6 ns).

In Fig. 10, we show the time profiles of $^3BP^*$, BPH·, and IP's, which were obtained by the analysis of the observed spectra in Fig. 9 into these components. The initial yields of $^1IP_{com}$, $^1IP_{enc}$, and $^3BP^*$ were determined by the femtosecond laser photolysis, respectively. In addition, the reaction pathways have been elucidated and their rate constants have been determined respectively for $^3BP^*$, $^3IP_{enc}$, and $^1IP_{com}$. Hence, in principle, informations on the reactions of $^1IP_{enc}$ can be obtained by subtracting from the observed results the contributions from the reaction between $^3BP^*$ and DEA and that of $^1IP_{com}$ on the basis of their initial yields and time dependences. In the actual analysis of the time profiles of $^1IP_{enc}$, we employed the curve-fitting procedure where the lifetime and the reaction yields were varied as parameters. The solid lines in Fig. 10 were calculated curves by assuming that the lifetime, the reaction yield of the proton transfer, and the ionic dissociation yield of $^1IP_{enc}$ were 350 ps, 0.14, and 0.50, respectively. The solid curves for IP's and BPH· in Fig. 10 include the contributions from $^3IP_{enc}$ and $^1IP_{com}$. As shown in Fig. 10, the experimental results are reproduced by the calculated time dependences, and further, parameters for $^1IP_{enc}$ are almost independent of the DEA concentration as shown in Table 2. The averaged lifetime, reaction yields for the proton transfer, ionic dissociation, and charge recombination of $^1IP_{enc}$ were 343 ps, 0.15, 0.48, and 0.37, respectively.

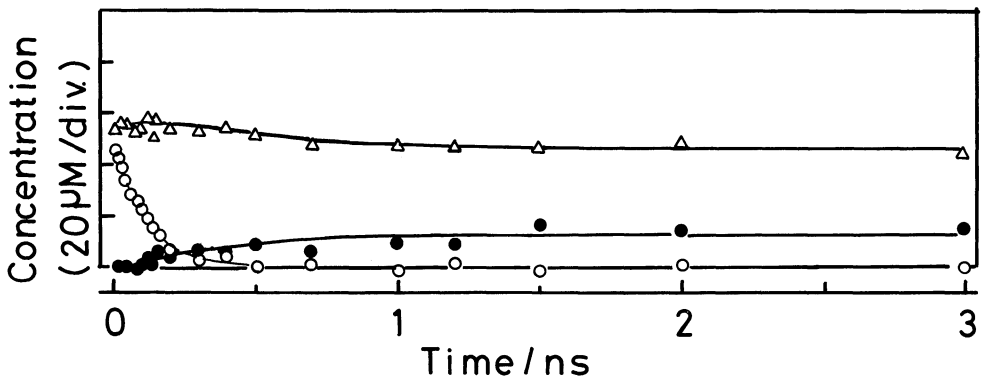

Fig. 10. Time profiles of $^3BP^*$ (○), BPH· (●), and BP^- and DEA^+ (△) of BP (0.01 M)–DEA (0.6 M) system in acetonitrile solution excited with a picosecond 355 nm laser pulse.

Table 2. Properties of the Singlet Ion Pair, $^1(BP^-\cdots DEA^+)_{enc}$, in Acetonitrile Solutions with Various Concentrations of DEA. τ: Lifetime, ϕ_{PT} and k_{PT}: Reaction Yield and Rate Constant of the Proton Transfer, ϕ_{ID} and k_{ID}: Reaction Yield and Rate Constant of the Ionic Dissociation, ϕ_{CR} and k_{CR}: Reaction Yield and Rate Constant of the Charge Recombination

[DEA]/M	τ/ps	ϕ_{PT}	ϕ_{ID}	ϕ_{CR}	k_{PT}/s^{-1}	k_{ID}/s^{-1}	k_{CR}/s^{-1}
0.3	350	0.15	0.45	0.40	4.3×10^8	1.3×10^9	1.1×10^9
0.6	350	0.14	0.50	0.36	4.0×10^8	1.4×10^9	1.0×10^9
1.0	330	0.15	0.50	0.35	4.6×10^8	1.5×10^9	1.1×10^9
Average	(343±9)	0.15±0.005	0.48±0.024	0.37±0.021	$(4.3\pm0.044)\times10^8$	$(1.4\pm0.094)\times10^9$	$(1.1\pm0.04)\times10^9$

4. Absorption Maximum of BP^- and the Structure of IP Including the Surrounding Solvents. Peters et al. reported the time-dependent blue-shift of the absorption spectrum of BP^- in the photoreduction process of excited BP with amines including DEA and they concluded that this shift was due to the structural change of the IP from the solvent-separated IP(SSIP) to the contact IP(CIP) based on the postulate that the ET reaction proceeded exclusively between $^3BP^*$ and amines.[12] As shown in Fig. 9, it was observed also in the present study that the peak position of BP^- absorption band gradually shifted from 730—740 nm to 700—710 nm region with increase of the delay time after the excitation. However, as we have pointed out in the previous sections of this paper and in the previous paper on the reduction of excited BP with DMA,[17,18] the contributions of both $^1IP_{com}$ and $^1IP_{enc}$ to the observed spectra should be taken into account for the elucidation of this spectral shift. The wavelength of the absorption peak of BP^- in $^1IP_{com}$ which decays with the time constant of (93±5) ps, was 740 nm as indicated in Fig. 6, and was different from those of $^3IP_{enc}$ and free BP^-.

In order to clarify whether the spectral shift is the intrinsic one caused by the structural change of IP or the apparent one arising from the disappearance of $^1IP_{com}$, we plotted the spectrum of BP^- obtained by subtracting the contribution of the spectrum due to $^1(BP^-\cdots DEA^+)_{com}$ overlapping those of $^1(BP^-\cdots DEA^+)_{enc}$ and $^3(BP^-\cdots DEA^+)_{enc}$ considering its fraction determined by the analysis of the time profiles of those species and its lifetime (dotted lines in Fig. 9). It is clear that the spectrum from which the contribution of $^1(BP^-\cdots DEA^+)_{com}$ was removed showed an absorption maximum around 700—720 nm although a rather broad spectrum gradually evolved into a sharper one with increase of the delay time after the excitation. From this result, we can conclude that the time dependent spectral shift was caused mainly by the disappearance of the spectrum due to $^1(BP^-\cdots DEA^+)_{com}$. This result is similar to that observed previously in the case on BP–DMA in acetonitrile solution.[17,18]

The fact that the absorption maximum of $^1IP_{com}$ is different from those of $^1IP_{enc}$, $^3IP_{enc}$, and free BP^- in both BP–DMA and BP–DEA systems may be ascribed to the difference of the structure of IP such as the mutual distance and orientation between BP^- and amine cation including the surrounding solvents. The present results clearly indicate that such assignment of the longer wavelength absorption to the SSIP and shorter one to the CIP as made by Peters et al.[12] is erroneous. Since the absorption maximum of the free BP^- was rather close to those of $^1IP_{enc}$ and $^3IP_{enc}$, ca. 700—720 nm, the structure of the solvation surrounding the BP^- in these IP_{enc}'s seems to be rather similar to those of the free BP^-. Hence, it is reasonable to assign the absorption maximum at 740 nm to the compact IP or CIP state of BP^- and amine cation and that at 700—720 nm to a more or less loose IP (LIP) or SSIP and solvated free ion state.

The above assignment is also supported by the recent investigations which demonstrate the large difference in the dynamic behaviors of IP's of various donor acceptor systems depending on the mode of their production.[2,20,28] In these studies, charge recombination (CR) rate of IP produced by the excitation of the CT complex and its dependence on the energy gap between the IP state and the ground state, $-\Delta G^\circ_{ip}$, have been examined in the case of various CT complexes covering a wide range of the energy gap by using femtosecond and picosecond laser photolysis. By these investigations, it has been revealed that the CR rate of IP produced by the CT complex excitation shows an essentially different energy gap dependence from the bell shaped one obtained in the case of IP formed by charge separation at encounter in the fluorescence quenching reaction.[2-4,20,28] Further, the CR rate of IP produced by the CT complex excitation has been confirmed, in general, to be greater than that of IP formed by charge separation at encounter for the same donor (D) and acceptor (A) pair in acetonitrile.[20] From these and related findings, it has been also suggested that the structure of IP's including the surrounding solvent is different from each other; the CIP probably with no intervening solvent molecule between A^- and D^+ would be produced in the case of the excitation of the CT complex, while LIP or SSIP with intervening solvent molecules between A^- and D^+ may be formed in the CS at encounter in the fluorescence quenching reaction. Moreover, from the results of those investigations, it has been concluded that the structures of these IP's could be maintained at least during several hundreds of picoseconds.[2-4,20,28]

Table 3. Dependence of the Reaction Rate Constants of the Ion Pairs upon the Mode of Its Production

	k_{PT}/s^{-1}	k_{ID}/s^{-1}	k_{CR}/s^{-1}
$^3(BP^-\cdots DEA^+)_{enc}$	7.3×10^8	2.1×10^9	
$^1(BP^-\cdots DEA^+)_{enc}$	4.3×10^8	1.4×10^9	1.1×10^9
$^1(BP^-\cdots DEA^+)_{com}$	$\ll10^8$	1.4×10^9	9.3×10^9
$^3(BP^-\cdots DMA^+)_{enc}$	5.4×10^9	1.4×10^9	
$^1(BP^-\cdots DMA^+)_{enc}$	6.6×10^8	9.5×10^8	5.8×10^8
$^1(BP^-\cdots DMA^+)_{com}$	$\ll10^8$	$\leqslant4\times10^8$	1.1×10^{10}

The dependence of the CR rate of IP on its mode of the production as observed in the present study on BP–DEA system as well as BP–DEA system is similar to those observed in the case of the above described various singlet IP's. In addition, we have confirmed that the relation between the CR rate and $-\Delta G^\circ_{ip}$ observed for $^1IP_{com}$ as well as $^1IP_{enc}$ in the BP–DEA and BP–DMA systems is also quantitatively in agreement with that predicted by the experimental results on various singlet IP's covering a wide range of $-\Delta G^\circ_{ip}$.[2-4,20,28] From these results regarding the $-\Delta G^\circ_{ip}$ dependence of the CR rate, the behaviors of the present $^1IP_{com}$ and $^1IP_{enc}$ are considered to be typical of the IP's produced by the excitation of the CT complex and via the ET reaction at encounter collision in the fluorescence state, respectively. By integrating the experimental results on the absorption maxima of the spectrum of BP^- in various kinds of IP's and the energy gap dependence of the CR rate of BP–DEA as well as BP–DMA IP systems, it is reasonable to assign the absorption maximum at 740 nm to the contact or compact IP state of BP^- and amine cation and that at 700—720 nm to LIP or SSIP and solvated free ion state.

5. Difference of the Reactivity between IP's Depending on the Mode of the Production. In Table 3, we list the rate constants of the proton transfer, k_{PT}, the ionic dissociation, k_{ID}, and the the charge recombination, k_{CR}, for the three kinds of IP's, $^1IP_{com}$, $^1IP_{enc}$, and $^3IP_{enc}$. In this table, the results on the IP's of BP–DMA system[17,18] are included also for the purpose of comparison. The CR rate constant of $^3IP_{enc}$ is not listed in this table, since this rate constant is very small, and hence, its quantitative determination was difficult. In both systems, clear difference of each rate constant depending on the mode of the production of the IP was observed. This result indicates that the structure of the IP is different from each other and it is approximately kept during the lifetime of the IP.

Although the rate constant of each process such as the ionic dissociation, the charge recombination, and the proton transfer is different between $(BP^-\cdots DEA^+)$ and $(BP^-\cdots DMA^+)$, the dependence of the rate constant on the mode of the production of the IP is very similar. The k_{PT}, of $^3IP_{enc}$ is the largest among these three kinds of IP's and the yield of BPH· radical of $^1IP_{com}$ was practically zero for both systems. Since the dependence of the rate constant on the production mode of the IP, $(BP^-\cdots DEA^+)$, is very similar to that of $(BP^-\cdots DMA^+)$, the interpretation in the previous paper[17,18] seems applicable also to the present result. In the following, we briefly discuss the difference of the reactivity between different IP's.

5. (a) The Difference of the Reactivity between the Singlet IP's Depending on the Mode of Their Production. In general, the geometric requirement for the proton or the hydrogen atom transfer processes seems to be more severe compared to that for the electron transfer reaction, since the conformational requirement for the latter process is dependent on the electronic molecular orbital spreading over a rather wide region, while the sites for the transfer of proton or hydrogen in the donor and the acceptor are limited within the narrow region. Hence, the difference in the structure of the IP such as the orientation and the distance seems to strongly affect the proton transfer probability.

As we have discussed in the interpretation of the spectral shift of BP^- absorption indicated in Fig. 9, $^1IP_{com}$ between BP and DEA as well as DMA may have quite different structures including the solvation from those of IP_{enc}. As a consequence of this difference in the structure, the reactivity of $^1IP_{enc}$ may be quite different from that of $^1IP_{com}$. At the present stage of the investigation, it is rather difficult to determine the precise structure of the IP composed of two molecules. However, it is strongly suggested that the initial structure of $^1IP_{com}$, especially the orientation of D^+ and A^- in the IP, is quite different from those of IP_{enc}'s. In addition, from the $-\Delta G^\circ_{ip}$ dependence of the CR rate, it is suggested that the $^1IP_{com}$ between BP and DEA or DMA has a rather rigid structure where the ions cannot reorient to take a suitable structure for the proton transfer before the recombination, while $^1IP_{enc}$ produced by the electron transfer between $^1BP^*$ and the amine at encounter has a more or less loose structure and is long-lived to form the suitable geometry for ketyl radical formation.

5. (b) The Difference of the Reactivity between $^3IP_{enc}$ and $^1IP_{enc}$. The reaction mechanism of the ketyl radical formation in the case of BP–DEA and –DMA systems in acetonitrile solutions has been confirmed to be the successive one of the IP formation followed by the proton transfer not only in the case of $^3BP^*$ but also $^1BP^*$. However, reaction rate constants in $^3IP_{enc}$ and $^1IP_{enc}$ are different from each other. The large difference of the charge recombination rate constant, k_{CR}, between two kinds of IP's can be ascribed to the difference of the spin multiplicity of the IP. On the other hand, the rate constant of the proton transfer, k_{PT}, of $^3IP_{enc}$ is larger than that of $^1IP_{enc}$, which cannot be ascribed solely to the difference of the spin multiplicity. This difference of k_{PT} between the two kinds of IP's may be related to the difference in the structure of the IP such as the mutual distance and orientations of ions in the pair including the surrounding solvents. Although it is

rather difficult at the present stage of the investigation to give any definite conclusion on the structures of these IP's, it is plausible that the IP produced by the ET reaction between ^{1}BP* and the amine has a more specific structure since the ET process is mainly due to the very rapid non-stationary reaction between the neighboring pair and, as a consequence, the shorter mutual distance and some specific orientation between the pair may be favorable for the reaction, leading to somewhat different IP structures from those produced via the stationary diffusion process. The difference in the electronic structure of ^{1}BP* from ^{3}BP* may play also some role in determining the mutual configurations favorable for ET between donor and acceptor at the encounter.

Summarizing above results and discussion on the difference of reactivity between ^{1}IP's and that between IP_{enc}'s, it may be concluded that the difference of the reactivity depending on the mode of the production of IP is related mainly to the difference of the mutual orientation of D^+ and A^- in the IP arising from the initial mutual geometry between the BP and amine undergoing the photoinduced CT or ET reaction. The relation between the distance dependence of the ET reaction and that of the intra-IP PT process and its consequence on the final hydrogen abstraction yield will be discussed in the next section.

6. The Difference of the Reactivity of Ion Pairs Depending on the Oxidation Potential of the Amine. In addition to the difference of the reactivity of the IP depending on the mode of the production, a large difference of the reactivity of $^3IP_{enc}$ was also observed between BP–DMA and BP–DEA systems. In order to clarify factors causing this difference, we have investigated photoreduction processes of BP– *N,N*-diethyl-*p*-toluidine (*p*-DET) and BP– *N*-methyldiphenylamine (MDPA) systems. We have selected these tertiary amines on the following reasons. First, the reaction mechanisms for these tertiary amines are all consecutive one of Scheme 2. Second, molecular structures of these tertiary amines are rather close to one another and have different oxidation potentials; MDPA: 0.86 V (vs. S.C.E), DMA: 0.76 V, DEA: 0.72 V, and *p*-DET: 0.69 V.[31] Although the difference of the reactivity depending on the mode of the IP production, i.e. the difference among $^3IP_{enc}$, $^1IP_{enc}$, and $^1IP_{com}$, was observed also in BP–*p*-DET and –MDPA systems[31,32] just as in BP–DEA and BP–DMA systems, we concentrate our discussion on the reduction process of ^{3}BP*.

In Fig. 11, we show transient absorption spectra of BP (0.01 M) –*p*-DET (0.05 M) system in acetonitrile solution excited with a picosecond 355 nm laser pulse. The concentration of the amine (0.05 M) was low enough to selectively observe the dynamic behaviors of ^{3}BP*. With increase of the delay time, the transient absorption spectrum due to ^{3}BP* which appeared immediately after excitaion gradually decays together with the increase of

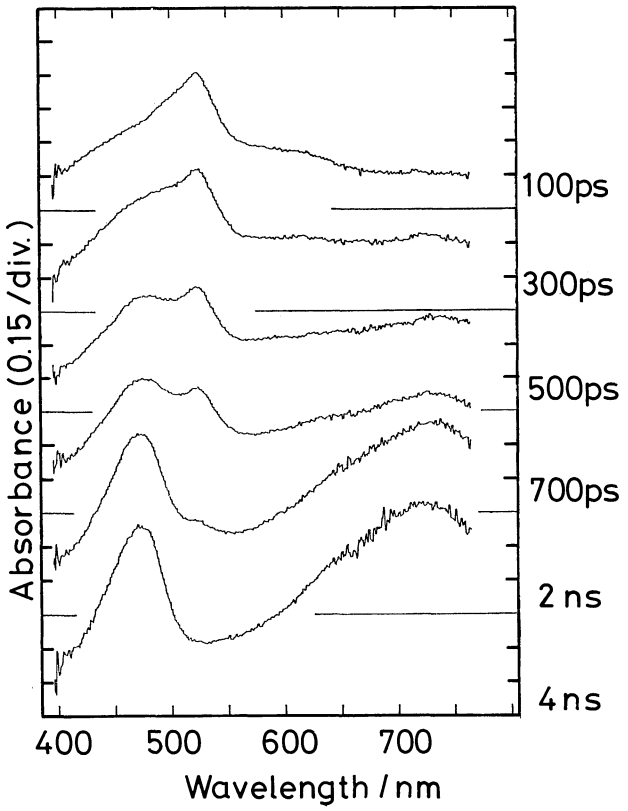

Fig. 11. Time-resolved transient absorption spectra of BP (0.01 M)–*p*-DET (0.05 M) system in acetonitrile solution, excited with a picosecond 355 nm laser pulse.

the absorbance at 700—720 nm (BP^-), and at 480 nm (*p*-DET^+). The absorbance due to BP^- and *p*-DET^+ reaches plateau value at 2—3 ns after the excitation and further evolution of the absorbance was not observed. From this result and those of the previous experiments,[9] the ionic species observed at a few ns after the excitation may be assigned to free ions. The yield of the free ions from ^{3}BP* was obtained to be 0.95±0.05 from the analysis of transient spectra in Fig. 11, where no ketyl radical formation was observed. Since neither decay process of the IP nor the formation of the ketyl radical was observed, it was not possible to determine the lifetime of $^3IP_{enc}$ by the present experiment. Hence, we estimate the lifetime and the reaction rate constants in the following manner. The rate constant for the ionic dissociation process of IP's of various donors and acceptors produced by ET at encounter in acetonitrile at room temperature (ca. 20 °C) has been determined to be $(0.5—2)\times10^9$ s^{-1}.[20,28] As listed in Table 3, k_{ID} for $^3(BP^-\cdots DEA^+)_{enc}$ and that for $^3(BP^-\cdots DMA^+)_{enc}$ were also in this range. Since the yield of the ionic dissociation of the $^3(BP^-\cdots p\text{-}DET^+)_{enc}$ was 0.95±0.05, the lifetime of the IP was estimated to be $\geqslant$500 ps assuming the similar k_{ID} value. Since the ketyl radical formation was not recognized, the rate constant for the proton transfer is estimated to be $\ll 2\times10^8$ s^{-1}. Anyhow, summarizing

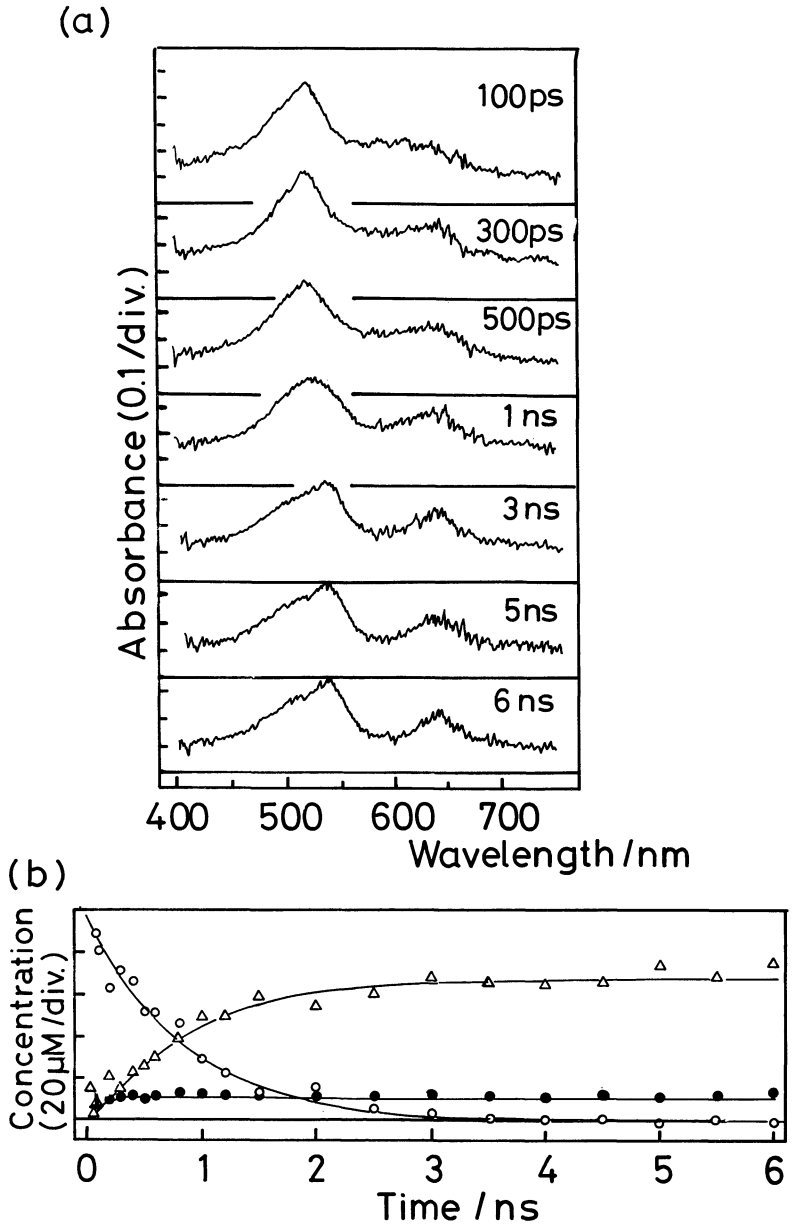

Fig. 12. a) Time-resolved transient absorption spectra of BP (0.01 M)–MDPA (0.07 M) system in acetonitrile solution, excited with a picosecond 355 nm laser pulse. b) Time profiles of ^{3}BP* (○), BPH· (△), and BP$^-$ and MDPA$^+$ (●) of BP (0.01 M)–MDPA (0.07 M) system in acetonitrile solution excited with a picosecond 355 nm laser pulse (see text). Solid lines are calculated curves based on Scheme 2 (see text).

above results on the reduction process of ^{3}BP*-*p*-DET system, it may be concluded that the decrease of the yield of BPH· is attributable to the decrease of k_{PT}. This result indicates that, k_{PT} of $^3IP_{enc}$ between BP and the tertiary aromatic amine decreases with the decrease of the oxidation potential of the amine.

In order to confirm the effect of the oxidation potential of the amine on k_{PT} of $^3IP_{enc}$, the photoreduction process of BP–MDPA system was also investigated. Fig. 12(a) shows transient absorption spectra of BP(0.01 M)–MDPA (0.07 M) in acetonitrile excited with a picosecond 355 nm laser pulse. Although the formation of $^1IP_{com}$ and $^1IP_{enc}$ was found to increase also in this system with increase of [MDPA],[32] contributions from these IP's to the observed spectra of ionic species in Fig. 12(a) is very little. The transient absorption spectra due to ^{3}BP* observed immediately after the excitation gradually evolved in time into those of MDPA$^+$ at 645 nm, BP$^-$ at 700—720 nm and BPH· at 545 nm. In Fig. 12(b), we exhibit the time profiles of ^{3}BP*, BPH·, and the IP.

Table 4. Dependence of the Reaction Rate Constants of the Triplet Ion Pairs upon Their Oxidation Potentials

Amine	MDPA	DMA	DEA	*p*-DET
Oxidation potential/V (vs. S.C.E.)	0.86	0.76	0.72	0.69
Lifetime of $^3IP_{enc}$/ps	90	140	290	(>500)
k_{PT}/s^{-1}	8.0×10^9	5.4×10^9	7.3×10^8	($\ll2\times10^8$)
k_{ID}/s^{-1}	1.1×10^9	1.4×10^9	2.1×10^9	(2×10^9)

Solid lines indicate the calculated curves based on the consecutive mechanisms (Scheme 2), similar to those indicated in Figs. 2 and 4. The lifetime of $^3(BP^{-}\cdots MDPA^{+})_{enc}$ was obtained to be 90 ps and the reaction yields of the proton transfer and the ionic dissociation were obtained to be 0.72 and 0.10, respectively. These values were confirmed to be almost independent of [MDPA].[32]

In Table 4, collected are the obtained values of the lifetime, k_{PT} and k_{ID} of $^3IP_{enc}$ of BP–tertiary aromatic amine systems in acetonitrile. This table shows clear dependence of each rate constant, especially k_{PT}, on the oxidation potential of the amine. This dependence of k_{PT} on the oxidation potential of the aromatic tertiary amine seems to indicate the different structure of the IP depending on the oxidation potential of the amine and seems to be closely related to the problems of the energy gap dependence of the ET reaction. Qualitatively speaking, the rate of the photoinduced ET reaction in polar solutions is regulated by:[33]

(a) Frank–Condon factor for the ET process which is related to the energy gap ($-\Delta G°$) between the initial and final state of ET, (b) the reorganization energy (λ) including the intramolecular vibrational modes and the polarization of the solvent surrounding D and A, (c) the solvent dynamics, and (d) the electronic interaction responsible for ET which depends on mutual distance and orientations between D and A. When the factor (d) is not very strong and is not much different throughout a series of D, A systems, the ET rate may be determined mainly by the factor (a) and (b).

The CR decay rate constant, k_{CR}, of LIP or SSIP formed by CS at encounter in the fluorescence quenching reaction[2,3,28] as well as the phosphorescence quenching reaction[34] has been confirmed to show bell-shaped energy gap dependence. These energy gap dependences are predicted by the usual theories on the ET reaction. On the other hand, the CS rate constant, k_{CS}, at encounter in the luminescence quenching reaction rises steeply around zero energy gap and becomes diffusion-limited at favorable $-\Delta G°$ regions, while no inverted effect has been experimentally confirmed yet. We have evaluated the k_{CS} values in the diffusion-limited $-\Delta G°$ regions by measuring the transient effect in the fluorescence quenching reaction of a series of D, A systems in acetonitrile solutions and have demonstrated that the $-\Delta G°$ dependence of k_{CS} in this top region is rather flat.[35] Such $-\Delta G°$ dependence of k_{CS} in the top region can be interpreted by assuming the change of the ET distance depending on the change of $-\Delta G°$ value.[35,36] That is, for larger $-\Delta G°$ value, CS at a little larger distance is favorable because λ becomes larger at larger D, A distance,[36] which makes the $-\Delta G°$ dependence of k_{CS} broader than that expected from the simple theoretical consideration.[37] We have made quantitative theoretical calculations on this problem, in which we have shown that the observed $-\Delta G°$ dependence of k_{CS} and k_{CR} can be interpreted by assuming D, A distance distributions depending on $-\Delta G°$ values in the CS reaction and also nonlinear polarization of solvent around ions.[36,38]

Along these theoretical treatments, it is expected, for the PT process following the ET reaction, that the PT rate should be drastically slowed down with the increase in the energy gap for the CS reaction in the condition where the orientation of BP^- and AH^+ and the surrounding solvation structure of IP are similar and the $-\Delta G°$ value for the CS reaction is relatively large. In other words, the increase in the inter-ionic distance in the geminate IP with increase of the energy gap for the CS reaction affects the subsequent PT rate to a great extent since the rate for the PT process is much more severely dependent on the mutual distance.

The present result of the dependence of k_{PT} of $^3IP_{enc}$ on the oxidation potential of the amine is in accordance with the above considerations on the mechanism of the energy gap dependence of k_{PT}. The inter-ionic distance in those BP–amine ^{3}LIP will become longer to a small extent with decrease of the oxidation potential of the amine and it seems to be kept until the proton transfer taking place in competition with the ionic dissociation. The k_{PT} will decrease with decrease of the amine oxidation potential due to the increase of the proton transfer distance.

The effect of the energy gap for the CS reaction on the PT rate which is attributable to the difference in the inter-ionic distance may be expected also in the course of the $^1IP_{enc}$ formation since it is actually observed for $^3IP_{enc}$. However, because the ET between ^{1}BP* and the amine is restricted rather severely to the pairs in the short range owing to the very short life of ^{1}BP*, such effect of the energy gap in the CS reaction will be small. Actually, k_{PT} in the $^1IP_{enc}$ does not show such energy gap dependence, but rather similar to each other for the series of ^{1}BP*–DEA, –DMA, and –MDPA systems ($k_{PT}=4.3\times10^8\ s^{-1}$, $6.6\times10^8\ s^{-1}$, and $6.0\times10^8\ s^{-1}$, respectively).

7. The Different Reaction Mechanism Depending on the Nature of the Amine. As discussed above, the mechanism of the hydrogen abstraction of ^{3}BP* from tertiary aromatic amines in acetonitrile solution is the successive reaction as given by the Scheme 2, while the hydrogen abstraction process of ^{3}BP* from primary and secondary amines such as aniline, DPA, *N*-methylaniline, and *N*-ethylaniline was the direct abstraction competing with the production of the stable IP which did not undergo the intra-IP proton transfer.[16,31] This difference of the reaction mechanism depending on the structure of the amine might be related to the existence of weak hydrogen bonding interaction between π-electrons on oxygen of the excited BP and the hydrogen directly bonded to the nitrogen of the amine. The CT interaction and this weak hydrogen bonding interaction might to closely connected with each other and facilitate the hydrogen transfer process in the encounter collision.

On the other hand, the mechanism of the hydrogen abstraction of ^{3}BP* from DMA in 2-propanol is not the successive one but can be described by the direct abstraction mechanism. The difference of the mechanism depending on the solvent may be related to the following experimental results on the singlet IP's. Concerning the structure and dynamics of the molecular complex produced by the photoinduced CT or ET reaction, it was reported that the electronic state of the typical singlet exciplex system such as pyrene–DMA was strongly dependent on the nature of the solvent such as the polarity and ability of hydrogen bonding interaction.[39,40] This dependence on the nature of the solvent was not accounted for by assuming the mere stabilization of the single electronic state by the solvation but it is necessary to take into account the change of the electronic and geometrical structures of the complex depending on the nature of the solvent.[39,40] In addition, it was revealed that, in sufficiently polar solvents, the fluorescent exciplex and nonfluorescent solvated IP's were produced competitively, depending upon the solvent polarity, from the non-relaxed CT state immediately after the electron transfer between excited singlet state of pyrene and DMA.[41] Integrating those previous results and the present ones, it is suggested that the mutual geometry such as orientation and distance including the surrounding solvent at the encounter between the reactants strongly affect the subsequent behaviors of the very short-lived transient charge transfer or the IP state.

Summarizing these various mechanisms depending on the structures of the amine, the nature of solvent, and the oxidation potential of the amine as well as the production pathways of IP, it is indicated that the transient charge transfer interaction in a short-lived intermediate formed in the excited benzophenone–amine system is of crucial importance as the factor determining the reaction mechanism.

In relation to this problem, we are now investigating the system where mutual configurations are restricted by connecting BP and amine with the methylene chain, results of which will be published in a forthcoming paper.

The present work was partially supported by a Grant-in-Aid for Specially Promoted Research No. 6265006 from the Ministry of Education, Science and Culture to N. M.

References

1) N. Mataga, *Pure Appl. Chem.*, **56**, 1255 (1984).
2) N. Mataga, *Acta Phys. Pol., A*, **71**, 767 (1987).
3) N. Mataga, "Photochemical Energy Conversion," ed by J. R. Norris and D. Meisel, Elsevier, Amsterdam (1988), p. 32.
4) N. Mataga, H. Miyasaka, T. Asahi, S. Ojima, and T. Okada, "Ultrafast Phenomena VI," Springer-Verlag, Berlin (1988), p. 511.
5) A. Beckett and G. Porter, *Trans. Faraday Soc.*, **59**, 2038 (1963).
6) G. Porter and M. R. Topp, *Proc. Roy. Soc. (London), Ser. A*, **315**, 163 (1970).
7) S. G. Cohen, A. Parola, and G. H. Rarsons, *Chem. Rev.*, **73**, 1411 (1973), and references cited therein.
8) S. Arimitsu and H. Masuhara, *Chem. Phys. Lett.*, **22**, 543 (1973).
9) S. Arimitsu, H. Masuhara, N. Mataga, and H. Tsubomura, *J. Phys. Chem.*, **79**, 1255 (1975).
10) K. S. Peters, S. C. Felich, and C. G. Shaefer, *J. Am. Chem. Soc.*, **102**, 5701 (1980).
11) C. G. Shaefer and K. S. Peters, *J. Am. Chem. Soc.*, **102**, 7567 (1980).
12) J. D. Simon and K. S. Peters, *J. Am. Chem. Soc.*, **103**, 6403 (1981).
13) L. E. Manring and K. S. Peters, *J. Am. Chem. Soc.*, **107**, 6452 (1985).
14) M. Hoshino and H. Shizuka, *J. Phys. Chem.*, **91**, 714 (1987).
15) H. Hoshino and M. Kogure, *J. Phys. Chem.*, **93**, 728 (1989).
16) H. Miyasaka and N. Mataga, *Bull. Chem. Soc. Jpn.*, **63**, 131 (1990).
17) H. Miyasaka, K. Morita, M. Kiri, and N. Mataga, "Ultrafast Phenomena VII," Springer-Verlag, Berlin (1990), p. 498.
18) H. Miyasaka, K. Morita, K. Kamada, and N. Mataga, *Bull. Chem. Soc. Jpn.*, **63**, 3385 (1990).
19) H. Miyasaka, K. Morita, K. Kamada, and N. Mataga, *Chem. Phys. Lett.*, **178**, 504 (1991).
20) a) N. Mataga, Y. Kanda, T. Asahi, H. Miyasaka, T. Okada, and T. Kakitani, *Chem. Phys.*, **127**, 239 (1988); b) T. Asahi and N. Mataga, *J. Phys. Chem.*, **93**, 6575 (1989); c) T. Asahi and N. Mataga, *ibid.*, **95**, 1956 (1991).
21) H. Masuhara, N. Ikeda, H. Miyasaka, and N. Mataga, *J. Spectros. Soc. Jpn.*, **31**, 19 (1982).
22) H. Miyasaka, H. Masuhara, and N. Mataga, *Laser Chem.*, **1**, 357 (1983).
23) H. Miyasaka, S. Ojima, and N. Mataga, *J. Phys. Chem.*, **93**, 3380 (1989).
24) E. J. Land, *Proc. Roy. Soc. (London), Ser. A*, **305**, 457 (1968).
25) R. V. Bensasson and J.-C. Gramain, *J. Chem. Soc.,*

Faraday Trans. 2, **76**, 1801 (1980).
26) T. Shida, S. Iwata, and M. Imamura, *J. Phys. Chem.,* **78**, 741 (1974).
27) H. Hiratsuka, T. Yamazaki, Y. Maekawa, T. Hidaka, and Y. Mori, *J. Phys. Chem.,* **90**, 774 (1986).
28) N. Mataga, T. Asahi, Y. Kanda, T. Okada, and T. Kakitani, *Chem. Phys.,* **127**, 249 (1988), and references there-in.
29) J. D. Simon and K. S. Peters, *J. Am. Chem. Soc.,* **105**, 4875 (1983).
30) R. K. Huddleston and J. R. Miller, *Radiat. Phys. Chem.,* **17**, 383 (1981).
31) T. Miyasaka, K. Kamada, K. Morita, M. Kiri, and N. Mataga, to be published.
32) H. Miyasaka, K. Morita, M. Kiri, T. Nagata, and N. Mataga, to be published.
33) N. Mataga, "Perspective in Photosynthesis," ed by J. Jortner and B. Pullman, Kluwer Academic, Dordrecht (1990), p. 227.
34) T. Ohno, A. Yoshimura, and N. Mataga, *Bull. Chem. Soc. Jpn.,* **94**, 4871 (1990), and references there-in.
35) S. Nishikawa, T. Asahi, T. Okada, N. Mataga, and T. Kakitani, *Chem. Phys. Lett.,* in press.
36) T. Kakitani, A. Yoshimori, and N. Mataga, "Advances in Chemistry Series," "Electron Transfer in Inorganic, Organic and Biological Systems," ed by J. R. Bolton, N. Mataga, and G. McLendon, Am. Chem. Soc. (1991), Chap. 4; *idem*, to be published.
37) R. A. Marcus, *J. Chem. Phys.,* **24**, 966 (1956); R. A. Marcus and N. Sutin, *Biochim. Biophys. Acta,* **811**, 265 (1985).
38) A. Yoshimori, T. Kakitani, Y. Enomoto, and N. Mataga, *J. Phys. Chem.,* **93**, 8316 (1989), and reference there-in.
39) N. Mataga, T. Okada, and N. Yamamoto, *Chem. Phys. Lett.,* **1**, 119 (1967).
40) N. Mataga and M. Ottolengthi, "Molecular Association Including Molecular Complexes," ed by R. Foster, Academic Press, London (1979), p. 1.
41) Y. Hirata, Y. Kanda, and N. Mataga, *J. Phys. Chem.,* **87**, 1659 (1983).